Electronic Supplementary Material (ESI) for Soft Matter

Electronic Supplementary Information for the review

"The polyelectrolyte properties of chromatin"

by **N. Korolev, A. Allahverdi, A. P. Lyubartsev and L. Nordenskiöld**

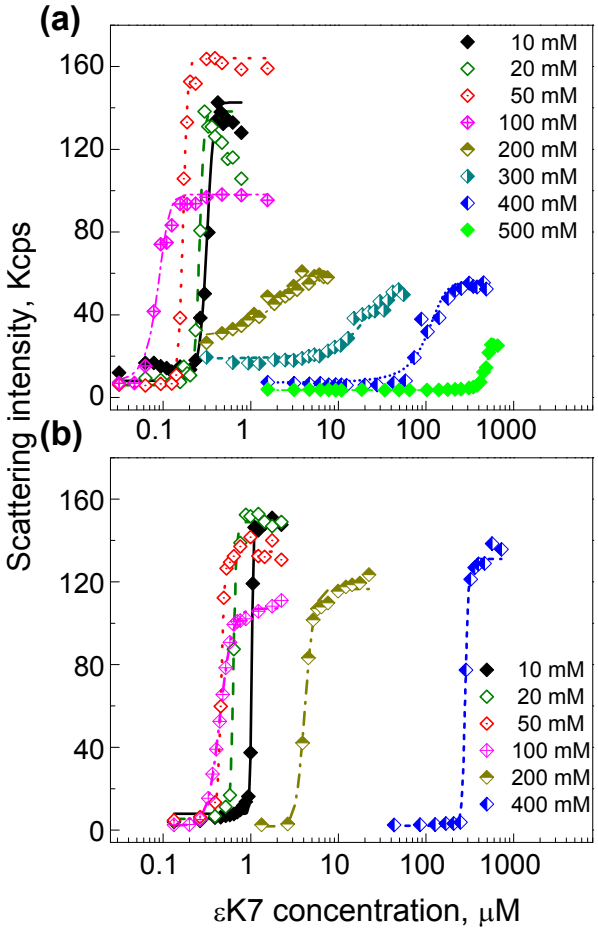

Figure S1. A series of titrations monitored by light scattering of plasmid DNA (**a**) and of the 12-177-601 nucleosome array (**b**) with the ε-oligolysine, εK7 (+8), in the presence of different concentrations of KCl. Points are experimental readings, curves are sigmoidal fitting of the data; all solutions contained 10 mM Tris·HCl, pH 7.5. For both array and pDNA, two groups of curves are seen. The first group is observed at low salt (below 100 mM KCl) with a relatively small shift to lower ligand concentration (C_L) with increase of KCl (salt-independent regime). The second group obtained at C_{KCl} > 100 mM shows a progressive shift to a higher ligand concentration with increase of C_{KCl} (salt-dependent regime). Similar features were observed for other cations with Z>+4 and for data obtained at higher DNA concentration (as in Fig. 3 of the main text) (1,2). A noticeable light scattering is observed in array solutions at $C_{KCl} \geq 200$ mM even in the absence of or presence of low concentration of cationic ligand (**a**) and can be explained by the array folding and aggregation caused by screening by monovalent salt, which occurs even in the absence of oligocation (3). The condensation of pure DNA is not possible under these conditions, therefore a similar effect was not observed (**b**). At 200-300 mM KCl, the ions not only screen DNA-DNA repulsion in the array but they also compete with the histone tails and with the oligocations. In the salt-dependent regime, this K^+ competition with oligocations counteracts array condensation and leads to an increase in EC_{50} (the critical concentration needed for 50% condensation).

Supporting text 1

Explanation of the salt dependence of EC_{50} in DNA and chromatin condensation by oligocations (equations 1 and 2 in the main text).

EC_{50} is the total concentration of the cationic ligand at the midpoint of oligocation titration to a solution of polyelectrolyte (DNA or chromatin) where the free energies of extended and condensed conformation of the polymer are equal. The ligand concentration is the sum of the concentrations of the ligand bound to the DNA and free in solution: $EC_{50} = C_L^{free} + C_L^{bound}$, where C_L^{free} and C_L^{bound} refer to the conditions at the midpoint of condensation. The value of C_L^{bound} is related to the degree of neutralization of polyelectrolyte charge by the ligand (N^L_{crit}) necessary to induce condensation at given concentration of monovalent salt. $C_L^{bound} = C_P \cdot N^L_{crit}/Z$ (where C_p is DNA concentration and Z is the ligand charge). Generally, $N_{crit} = N^L_{crit} + N^M_{crit}$, is the sum of the fractions of monovalent counterions, N^M_{crit} and cationic ligands, N^L_{crit}, bound per one phosphate and contribute to the screening of the polyelectrolyte at the midpoint of condensation. As it was established by Wilson and Bloomfield (4), N_{crit} is relatively constant and equal to 0.88-0.90 for double stranded (ds) DNA in water solution.

The free ligand concentration, C_L^{free} is dependent on the DNA binding affinity of the ligand: $C_L^{free} = K_d \cdot C_L^{bound}/C_P^{free}$. Here K_d is the dissociation constant of the ligand-DNA complex ($K_d = 1/K_b$, binding constant);, $C_P^{free} = C_P - Z \cdot C_L^{bound}$ is the concentration of free DNA; or more specifically, the concentration of DNA phosphate groups not neutralized by the oligocation. After a simple transformation the dependence of EC_{50} takes the form:

$$EC_{50} = N_{crit} \cdot [K_d/(1 - N^L_{crit}) + C_P]/Z \qquad (1)$$

Equation (1) is general and based on thermodynamic-stoichiometric considerations of the DNA-ligand binding equilibrium at the midpoint of condensation. At low concentration of monovalent salt, the contribution from L^{Z+} is dominant as it has been shown by experimental measurements of the composition of ions in condensed DNA (5). Furthermore, theoretical calculations using Manning counterion condensation theory (6) (see Supplementary Data of our recent work (2)) or Poisson Boltzmann theories (7) as well as Monte Carlo simulations supports these observations (8). Therefore, at low concentration of monovalent salt it is reasonable to assume $N_{crit} \approx N^L_{crit}$.

It is well established that oligocation-DNA (9-13) as well most of protein-DNA (14) interactions are strongly salt-dependent (11,13) with the dissociation (binding) constant showing a linear dependence in logarithmic coordinates, $\log K_d$ versus $\log C_{salt}$ (we use KCl in our work):

$$\log K_d = \log K_d(1M) + SK \cdot \log C_{KCl} = \log K_d(1M) + bZ \cdot \log C_{KCl} \qquad (2) \text{ or}$$

$$K_d = K_d(1M) \cdot C_{KCl}^{bZ} \qquad (2a).$$

Here $K_d(1M)$ is the value of K_d extrapolated to $C_{KCl} = 1$ M, the term which accumulates all non-electrostatic effects of oligocation-DNA interactions (9,10,12,13); $SK = d\log K_d/d\log C_{KCl}$

≈ bZ is the slope of the $\log K_d$-$\log C_{salt}$ dependence; b is the thermodynamic degree of binding of the monovalent cation binding to the DNA polyion per negative phosphate charge. Estimates of b for double-stranded dsDNA and synthetic polynucleotides in interaction with α-oligolysines and α-oligoarginines give similar values of b that are close to unity (b ≈ 0.9) (11,12). Consequently, the slope SK is steep and sensitive to the value of Z. Combining Eqs. (1) and (2a) gives the relation for EC_{50}:

$$EC_{50} = N_{crit}\cdot[K_d(1M)\cdot C_{KCl}{}^{bZ}/(1 - N_{crit}) + C_P]/Z \qquad (3)$$

The above result presents a simple and clear explanation of the observed two regimes in the dependencies of EC_{50} on monovalent salt concentration. Using the approximate value $N^L_{crit} \approx N_{crit} = 0.9$, Eq. (1) takes a very simple form: $EC_{50} = 0.1\cdot[10\cdot K_d + C_P]/Z)$. Hence, one can illustrate the conditions defining DNA condensation either in the salt-independent or the salt-dependent regime:

For the low salt concentration when there is little competition between the ligand and monovalent cations, $10K_d < C_P$ and EC_{50} is proportional to the DNA concentration and independent of monovalent salt (C_{KCl}). For the high salt regime when there is a considerable competition between the ligand and the monovalent cations, $K_d > C_P/10$ and EC_{50} is salt dependent and proportional to $C_{KCl}{}^{bZ}$. The region of transition depends largely on the DNA concentration and the charge of the ligand such that high DNA concentration and/or high ligand charge preserves the salt-independent regime. Equation (3) can be used to fit the experimental data with $K_d(1M)$ and b (in $SK = bZ$, with Z given by ligand charge) as only independent variables. In the case of available experimental results for $K_d(1M)$ and $SK = bZ$ it can be used to compare with prediction on the basis of independent experimental data.

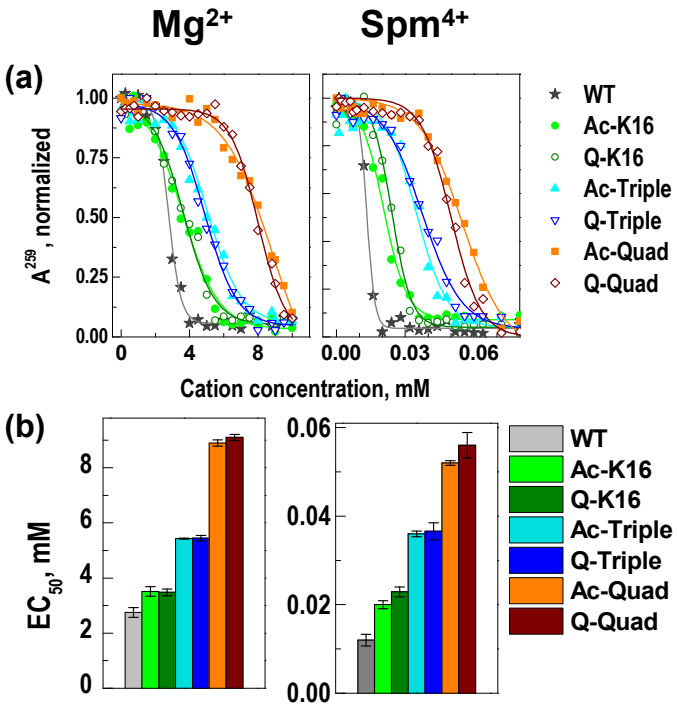

Figure S2. (**a**). Precipitation assay (PA) curves showing the absorbance, A^{260}, in the supernatant of different array solutions (10 mM Tris·HCl, pH 7.5; initial array concentration C_P = 151 μM of DNA) versus concentration of the added cations Mg^{2+} (left) and Spm^{4+} (right). Points are measured values (normalized relative to the A^{260} absorbance in the array solution without added cation); curves are sigmoidal fitting of the experimental data. (**b**) EC_{50} values of the 12-177-601 arrays with WT, acetylated and K→Q mutated histone H4 obtained for Mg^{2+} and Spm^{4+}. The type of the histone H4 construct used in the reconstituted 12-177-601 array is indicated to the right of the graphs. These PA data demonstrate that chromatin fiber self-association is insensitive to the nature of the charge alteration and follows the rules expected from a purely electrostatic model. Data adapted from ref (15).

Supporting text 2

Coarse-grained models of the nucleosome core particle (NCP) and nucleosome array describing electrostatic effects of flexible histone tails and explicit mobile ions.

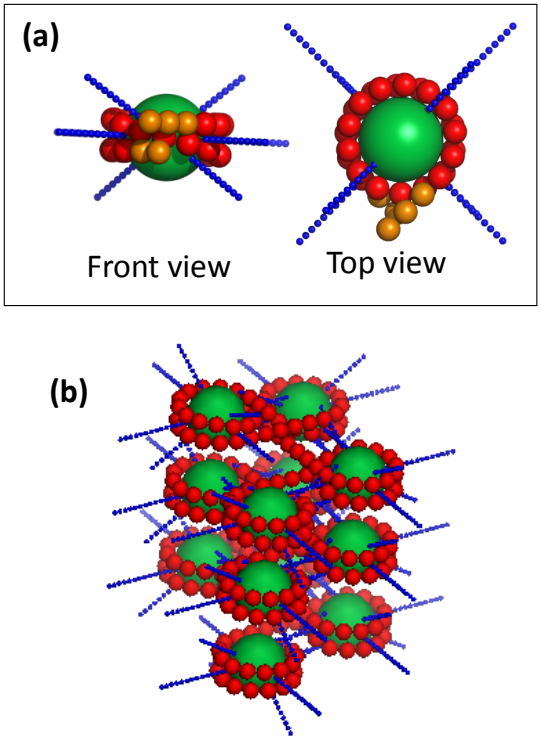

Figure S3. (**a**). The "Sphere-Bead" model of the nucleosome; partially neutralized DNA beads are red; fully charged beads modeling the linker DNA are orange. (**b**). Model of the "12-177" nucleosome array (initial configuration in the simulation cell). These models used to describe NCP-NCP interaction and nucleosome array folding in our recent work (3,15,16).

A coarse-grained nucleosome array model consisting of 12 nucleosomes was considered in papers (3,15) within the so-called sphere-bead model shown in Fig. S3 above. The nucleosome core particle was approximated as a combination of three types of particles. A central sphere represents the globular part of the histone octamer (HO). 25 particles model the nucleosomal DNA wrapped around the HO and 8 strings of connected beads describe the histone N-terminal tails with each bead representing one charge in the histone tail. Each DNA bead (of effective radius 1.0 nm) represents 6 bp DNA and were fixed on the surface of the central particle (of radius 3.5 nm) forming 1.75 superhelix mimicking DNA wrapping around the HO. The original –12e charge of each DNA bead is reduced to –9.44e (total charge –9.44e×25=–236e charge, which is equal to that of the sum of the charges on 147 bp DNA (–294e) plus the globular part of the histone octamer (+58e). This assumes partial neutralization of the DNA charge by the net positive charge of the HO core (see justification and discussion on charge distribution on the HO core in the supplementary material of our previous work (3)). In MD simulations of the nucleosomal array; the array model includes 12

NCPs connected to each other by 5 beads of DNA with −12e charge on each particle so these five beads mimics the length of linker DNA in the 12-177-601 nucleosome arrays experimentally studied in our in several other laboratories.

The histone tails were modeled as 8 strings of connected +1e charges of effective radius 0.25 nm and bond length 0.7 nm (17,18). The number of charged particles in each tail was 9, 14, 11, and 10 to match the charge of the H2A, H2B, H3 and H4 tails respectively. The described combination of the bead sizes and positioning closely represents the crystallographic structure of the NCP (19,20). Detailed description of the bond potentials as well as the long range (Coulombic) and short range (Lennard-Jones) force parameters is given in our earlier work.(3,18). Different arrangements of the tails have been tested including tailless NCPs as well as with changes in tail particle charge and size mimicking histone acetylations or K→Q mutations at the four lysines of the H4 tail (K5, K8, K12, and K16).

Langevin molecular dynamics simulations were carried out for a cubic simulation cell with a size of 40 nm containing 10 NCPs or one nucleosome array. Various counterions neutralizing the negative charge of the NCPs or array as well as added salts have been modeled explicitly. This simulation setup was found to allow satisfactorily reproduction the experimentally observed salt-dependent chromatin compaction and NCPs aggregation in the presence of Mg^{2+}, $CoHex^{3+}$, $spermidine^{3+}$ and $spermine^{4+}$ counterions (3,15). Qualitative agreement between experimental observations and MD simulations has been also reported for NCPs solutions where nucleosome core particle was modeled by simpler presentation that is histone octamer and nucleosomal DNA was approximated as single negatively charged particle (modelling flexible histone tails was the same) (17,18).

Sedimentation coefficient for arrays were calculated in the way described in (21) using the method developed by Bloomfield et al (22) following the Kirkwood approach (23). By neglecting the contribution of linker DNA, the sedimentation coefficient $S_{20,w}$ can be approximated as

$$S_{20,w} = S_1\left(1+\frac{R_1}{N}\sum_{i>j}\frac{1}{R_{ij}}\right)$$

where the summation is taken over all N=12 NCP pairs, R_{ij} is the distance between two nucleosomes, and parameters R_1 = 5.5 nm and S_1 = 11.1 Svedberg (S; 1 S = 10^{-13} sec) are adopted from previous works (24). From the array structures in the trajectories of the simulations, the S value as defined above averaged over the simulation, which corresponds to the experimentally observed sedimentation coefficient, is calculated.

References

1. Korolev, N., Zhao, Y., Allahverdi, A., Eom, K.D., Tam, J.P. and Nordenskiöld, L. (2012) The effect of salt on oligocation-induced chromatin condensation. *Biochem.Biophys.Res.Comm.*, **418**, 205-210.

2. Korolev, N., Berezhnoy, N.V., Eom, K.D., Tam, J.P. and Nordenskiöld, L. (2009) A universal description for the experimental behavior of salt-(in)dependent oligocation-induced DNA condensation. *Nucleic Acids Res.*, **37**, 7137–7150.
3. Korolev, N., Allahverdi, A., Yang, Y., Fan, Y., Lyubartsev, A.P. and Nordenskiöld, L. (2010) Electrostatic origin of salt-induced nucleosome array compaction. *Biophys. J.*, **99** 1896-1905.
4. Wilson, R.W. and Bloomfield, V.A. (1979) Counterion-induced condensation of deoxyribonucleic acid. A light-scattering study. *Biochemistry*, **18**, 2192-2196.
5. Korolev, N., Lyubartsev, A.P., Rupprecht, A. and Nordenskiöld, L. (2001) Competitive substitution of hexammine cobalt(III) for Na^+ and K^+ ions in oriented DNA fibers. *Biopolymers*, **58**, 268-278.
6. Manning, G.S. (1978) The molecular theory of polyelectrolyte solutions with application of the electrostatic properties of polynucleotides. *Q.Rev.Biophys.*, **11**, 179-246.
7. Rouzina, I. and Bloomfield, V.A. (1997) Competitive electrostatic binding of charged ligands to polyelectrolytes: practical approach using the non-linear Poisson-Boltzmann equation. *Biophys.Chem.*, **64**, 139-155.
8. Korolev, N., Lyubartsev, A.P., Nordenskiöld, L. and Laaksonen, A. (2001) Spermine: an "invisible" component in the crystals of *B*-DNA. A grand canonical Monte Carlo and molecular dynamics simulation study. *J.Mol.Biol.*, **308**, 907-917.
9. Mascotti, D.P. and Lohman, T.M. (1990) Thermodynamic extent of counterion release upon binding oligolysines to single-stranded nucleic acids. *Proc.Natl.Acad.Sci.U.S.A.*, **87**, 3142-3146.
10. Mascotti, D.P. and Lohman, T.M. (1993) Thermodynamics of single-stranded RNA and DNA interactions with oligolysines containing tryptophan. Effects of base composition. *Biochemistry*, **32**, 10568-10579.
11. Anderson, C.F. and Record, M.T. (1995) Salt-nucleic acid interactions. *Annu.Rev.Phys.Chem.*, **46**, 657-700.
12. Mascotti, D.P. and Lohman, T.M. (1997) Thermodynamics of oligoarginines binding to RNA and DNA. *Biochemistry*, **36**, 7272-7279.
13. Record, M.T., Zhang, W. and Anderson, C.F. (1998) Analysis of effects of salts and uncharged solutes on protein and nucleic acid equilibria and processes: a practical guide to recognizing and interpreting polyelectrolyte effects, Hofmeister effects, and osmotic effects of salts. *Adv.Protein Chem.*, **51**, 281-353.
14. Privalov, P.L., Dragan, A.I. and Crane-Robinson, C. (2011) Interpreting protein/DNA interactions: distinguishing specific from non-specific and electrostatic from non-electrostatic components. *Nucleic Acids Res.*, **39**, 2483–2491.
15. Allahverdi, A., Yang, R., Korolev, N., Fan, Y., Davey, C.A., Liu, C.F. and Nordenskiöld, L. (2011) The effects of histone H4 tail acetylations on cation-induced chromatin folding and self-association. *Nucleic Acids Res.*, **39**, 1680–1691
16. Liu, Y., Lu, C., Yang, Y., Fan, Y., Yang, R., Liu, C.-F., Korolev, N. and Nordenskiöld, L. (2011) Influence of histone tails and H4 tail acetylations on nucleosome–nucleosome interactions. *J.Mol.Biol.*, **414**, 749–764.
17. Korolev, N., Lyubartsev, A.P. and Nordenskiöld, L. (2006) Computer modeling demonstrates that electrostatic attraction of nucleosomal DNA is mediated by histone tails. *Biophys.J.*, **90**, 4305-4316.
18. Yang, Y., Lyubartsev, A.P., Korolev, N. and Nordenskiöld, L. (2009) Computer modeling reveals that modifications of the histone tail charges define salt-dependent interaction of the nucleosome core particles. *Biophys.J.*, **96**, 2082-2094.

19. Luger, K., Mader, A.W., Richmond, R.K., Sargent, D.F. and Richmond, T.J. (1997) Crystal structure of the nucleosome core particle at 2.8 Å resolution. *Nature*, **389**, 251-260.
20. Davey, C.A., Sargent, D.F., Luger, K., Maeder, A.W. and Richmond, T.J. (2002) Solvent mediated interactions in the structure of nucleosome core particle at 1.9 Å resolution. *J.Mol.Biol.*, **319**, 1097-1113.
21. Sun, J., Zhang, Q. and Schlick, T. (2005) Electrostatic mechanism of nucleosomal array folding revealed by computer simulation. *Proc.Natl.Acad.Sci.U.S.A.*, **102**, 8180-8185.
22. Bloomfield, V., Dalton, W.O. and Van Holde, K.E. (1967) Frictional coefficients of multisubunit structures. I. Theory. *Biopolymers*, **5**, 135-148.
23. Kirkwood, J.G. (1954) The general theory of irreversible processes in solutions of macromolecules. *J.Polym.Sci.*, **6**, 1-14.
24. Garcia-Ramirez, M., Dong, F. and Ausio, J. (1992) Role of the histone "tails" in the folding of oligonucleosomes depleted of histone H1. *J.Biol.Chem.*, **267**, 19587-19595.